Structure of the binuclear tetranitrosyl iron complexes with pyrimidin-2-yl of the μ_2-S type and the pH effect on its NO-donor ability in aqueous solutions*

N. A. Sanina, G. V. Shilov, S. M. Aldoshin, A. F. Shestakov, L. A. Syrtsova, N. S. Ovanesyan, E. S. Chudinova, N. I. Shkondina, N. S. Emel´yanova, and A. I. Kotel´nikov*

Institute of Problems of Chemical Physics, Russian Academy of Sciences, 1 prosp. Akad. Semenova, 142432 Chernogolovka, Moscow Region, Russian Federation. E-mail:sanina@icp.ac.ru sanina@icp.ac.ru

New binuclear tetranitrosyl iron complex with pyrimidin-2-yl of the μ_2-S type $[Fe_2(SC_4H_3N_2)_2(NO)_4]$ (**1**) was synthesized by the exchange reaction of thiosulfate ligands in the $[Fe(S_2O_3)_2(NO)_2]^{3-}$ anion for pyrimidin-2-yl ligands. The crystal structure of complex **1** was studied by single-crystal X-ray diffraction analysis. According to the X-ray diffraction data, pyrimidin-2-yl is coordinated to the iron atom in the thiol form. According to the quantum chemical calculations, the low stability of complex **1** is related to a possibility of formation of the coordination bond of the iron atom with the atom of the pyrimidine cycle of the ligand after NO group detachment. The ability of complex **1** to donate NO and the kinetics of its hydrolysis in aqueous solutions were studied by electrochemical analysis using sensor electrodes amiNO-700, by spectrophotometry in the pH interval from 6.0 to 7.76, and in the reaction with hemoglobin. Complex **1** is most stable in a neutral medium and more vigorously evolves NO in acidic and alkaline media.

Key words: NO donors, sulfur-nitrosyl iron complexes, pyrimidine-2-thiol, X-ray diffraction analysis, Mössbauer spectroscopy, nitrosyl hemoglobin.

It was found by numerous studies of the recent years that nitrogen monoxide (NO) is an important agent in bioregulation of diverse physiological processes.[1,2] This stimulates interest in the synthesis and study of new compounds that can easily transport NO to biological targets at physiological pH values[3] and serve a basis for the new generation of medicinals. Among these substances are thiolate nitrosyl iron complexes $[Fe_2(SR)_2(NO)_4]$, which are hydrolyzed similarly to *S*-nitrosothiols[4] and diazenium dialates[5,6] to form NO in protic media[7] and compose a new class of universal NO donors for pharmacological applications.[8—10] We have previously[7,11] established that without activation the iron sulfur-nitrosyl complexes decompose to evolve NO in protic media containing hemoglobin (Hb), and the reaction rate constant depend on the molecular structure of the complexes. Although in the most cases the exogenic NO donors are used at physiological pH values, the study of the dependence of these reaction rate constants on the pH of the medium is of considerable interest both from the viewpoint of stability of the NO donors during preparation and storage and obtaining important information on the mechanisms of nitrosylation reactions *in vivo*. In addition, the behavior *in vivo* of the sulfur-nitrosyl iron complexes at lowered pH values (for instance, in many tumors) requires detailed studies of the effect of the pH of the medium on the rate constant of NO evolution. This information is significant for pharmacological use of the iron-nitrosyl complexes as NO donors and also in the general aspect of chemical biology of NO.[12]

In the present work, we synthesized the new tetranitrosyl binuclear iron complex with pyrimidin-2-yl $[Fe_2(SC_4H_3N_2)_2(NO)_4]$ (**1**). The ligand in this complex is a metabolite widely used for the synthesis of new antitumor medicinals.[13—16]

The structure of synthesized complex **1** was studied by X-ray diffraction analysis, Mössbauer spectroscopy, and IR spectroscopy. The NO-donor activity of complex **1** in aqueous solutions was studied by the sensor electrode amiNO-700 at pH 6.0—7.7 and in its reaction with Hb. Quantum chemical calculations by the density functional B3LYP and PBE methods were performed for analysis of the electronic structure and reactivity of complex **1**.

Experimental

Commercial reagents $Na_2S_2O_3 \cdot 5H_2O$, KOH, and 2-mercaptopyrimidine (Aldrich) were used for the synthesis of complex **1**.

* Dedicated to Academician I. I. Moiseev on his 80th birthday.

Published in Russian in *Izvestiya Akademii Nauk. Seriya Khimicheskaya,* No. 3, pp. 560—571, March, 2009.

1066-5285/09/5803-0572 © 2009 Springer Science+Business Media, Inc.

Complex $Na_2[Fe_2(\mu_2\text{-}S_2O_3)_2(NO)_4] \cdot 4H_2O$ was synthesized by a known method.[17] All procedures on solution preparation, the reaction, and isolation of complex **1** were carried out in pure nitrogen. Absolute *n*-butyl alcohol and dichloromethane were purified according to earlier described procedures.[18] Solvent DMSO (reagent grade, Khimmed, Russia) was additionally purified by distillation at 10 Torr, collecting the fraction with b.p. 73—75 °C. Water was purified by successive distillation in a D-4 distillator and a Pyrex apparatus (pyrator Bi/Duplex (Germany)).

Serum hemoglobin MP Biomedicals, Germany), Sephadex G-25 (Pharmacia, Switzerland), sodium dithionite (Merck, Germany), $Na_2HPO_4 \cdot 6H_2O$, and $NaH_2PO_4 \cdot H_2O$ (MP Biomedicals, Germany) were used.

μ_2-*S*-[Bis(pyrimidine-2-thiolato)tetranitrosyliron] (1). An aqueous mixture of KOH (0.3 g, 7.5 mmol) with 2-mercaptopyrimidine (0.6408 g, 5 mmol) heated to 70 °C was added to an aqueous solution (20 mL) of a mixture of $Na_2S_2O_3 \cdot 5H_2O$ (0.496 g, 2 mmol) and $Na_2[Fe_2(S_2O_3)_2(NO)_4] \cdot 4H_2O$ (0.5740 g, 1 mmol). An argon flow was passed the reaction mixture for 10 min, and hot dichloromethane (40 mL) was added. The organic fraction was separated with a separating funnel and concentrated by evaporation to a volume of 10 mL. Then *n*-butyl alcohol (1—1.5 mL) was added, and the solution was concentrated to the complete removal of dichloromethane. A finely crystalline black powder with characteristic luster precipitated on cooling the solution to 20 °C. The precipitate was filtered off on a paper filter and dried in air (2—2.5 h). The yield of complex **1** was 0.27 g (51.0%).

Elemental analysis for the content of N, S, and Fe was carried out by electron probe microanalysis on an INCA Energy 450 energy disperse spectrometer. Calculations were performed using the INCA, version 4.07 program (Oxford Instruments Ltd., Great Britain) followed by the recalculation of the obtained results using the program package developed at the Institute of Experimental Mineralogy of the Russian Academy of Sciences. Carbon and hydrogen were determined at the Analytical Center of the Institute of Problems of Chemical Physics (Russian Academy of Sciences) using known procedures.[19] Found (%): C, 2.00; H, 1.17; Fe, 24.47; N, 23.83; S, 13.96. Calculated (%): C, 2.12; H, 1.34; Fe, 24.59; N, 24.68; S, 14.15.

X-ray diffraction experiment was carried out on a Bruker P-4 diffractometer (T = 200 K, λ(Mo-Kα) = 0.71073 Å, θ/2θ scan mode) with a black single crystal 0.12S0.05S0.02 mm in size. The crystallographic data and selected refinement parameters are given in Table 1. The structure was solved by a direct method. The positions and temperature parameters of non-hydrogen atoms were refined in the isotropic and then anisotropic approximation by the full-matrix least-squares method. The positions of hydrogen atoms were revealed from difference syntheses and refined in the isotropic approximation. All calculations were performed using the SHELXL-97 program package.[20] The coordinates of atoms are given in Table 2, and the interatomic distances and angles are listed in Table 3.

IR spectra were recorded on a Spectrum BX-II Fourier spectrometer. Samples were prepared as KBr pellets (1 mg of the studied substance per 300 mg of KBr). The IR spectrum of complex **1**, ν_{max}/cm^{-1}: 3472 (s), 1797 (vs), 1746 (vs), 1551 (m), 1425 (w), 1376 (w), 1191 (w), 1151 (m), 1070 (w), 811 (w), 774 (w), 739 (w), 629 (w), 550 (w); 480 (w); ν_{NO} 1797, 1746.

^{57}Fe Mössbauer absorption spectra were measured on a WissEl setup operating in the permanent acceleration mode. The source was ^{57}Co in the Rh matrix. The low-temperature spectra were measured using a CF-506 flow-type temperature-controlled helium cryostat (Oxford Instruments). Mössbauer spectra were processed by least squares assuming the Lorentzian shape of individual spectral components.

Theoretical study of the structure and decomposition of complex **1** was performed by the functional method in two versions: B3LYP in the 6-31G* basis set using the GAUSSIAN 98 program and the PBE method with the SBK pseudo-potential and the extended basis set using the PRIRODA program.[21] Comparing the energies of the optimized structures, we took into account the contribution of the zero-point energy. The

Table 1. Crystallographic data and experimental characteristics for complex **1**

Parameter	Value
Molecular formula	$C_8H_6Fe_2N_8O_4S_2$
Molecular weight	454.02
T/K	200(2)
Crystal system	Triclinic
Space group	$P\bar{1}$
a/Å	6.4170(10)
b/Å	7.6200(10)
c/Å	8.348(2)
α/deg	75.550(10)
β/deg	80.800(10)
γ/deg	85.200(10)
V/Å^3	389.79(12)
Z	1
ρ_{calc}/g cm^{-3}	1.934
μ/mm^{-1}	2.162
θ/deg	2.55—25.00
Total number of reflections	1607
Number of independent reflections	1214
R_{int}	0.0357
Number of reflections with $I > 2\sigma(I)$	912
GOOF	1.008
R ($I > 2\sigma(I)$)	$R_1 = 0.0356$, $wR_2 = 0.0732$
R (all reflections)	$R_1 = 0.0620$, $wR_2 = 0.0817$

Table 2. Coordinates of atoms in complex **1**

Atom	X	Y	Z	U_{eq}
Fe(1)	647(1)	11(1)	6476(1)	20(1)
S(1)	757(2)	−2382(1)	5301(1)	22(1)
N(1)	−1089(6)	−430(5)	8224(5)	25(1)
N(2)	3136(7)	359(5)	6593(4)	26(1)
O(1)	−2058(6)	−753(5)	9568(4)	42(1)
N(3)	−3093(7)	−3800(5)	6089(5)	29(1)
O(2)	4781(6)	545(5)	6940(5)	45(1)
C(1)	−1254(8)	−3818(6)	6605(5)	22(1)
N(5=4)	−588(7)	−4840(5)	7986(5)	32(1)
C(4)	−1992(10)	−5995(7)	8941(7)	36(1)
C(3)	−3939(9)	−6135(7)	8538(6)	30(1)
C(2)	−4428(10)	−5005(7)	7101(7)	34(1)

Table 3. Measured and calculated interatomic distances (d) and angles (ω) in complex **1**

Parameter	Experiment	Calculation	
		B3LYP	BBE
Bond	d/Å		
Fe(1)—N(2)	1.663(4)	1.630	1.657
Fe(1)—N(1)	1.668(4)	1.630	1.657
Fe(1)—S(1)$^{\#1}$	2.257(1)	2.220	2.240
Fe(1)—S(1)	2.267(1)	2.220	2.240
Fe(1)—Fe(1)$^{\#1}$	2.727(1)	2.560	2.664
N(1)—O(1)	1.170(5)	1.169	1.172
N(2)—O(2)	1.166(5)	1.169	1.172
S(1)—C(1)	1.800(5)	1.806	1.828
N(3)—C(1)	1.317(6)	1.334	1.339
N(3)—C(2)	1.343(6)	1.338	1.343
C(1)—N(5)	1.331(6)	1.333	1.339
N(5)—C(4)	1.333(6)	1.338	1.343
C(4)—C(3)	1.364(8)	1.394	1.398
C(3)—C(2)	1.356(8)	1.394	1.398
Angle	ω/deg		
N(2)—Fe(1)—N(1)	119.2(2)	116.0	117.0
N(2)—Fe(1)—S(1)$^{\#1}$	110.8(1)	109.5	109.1
N(1)—Fe(1)—S(1)$^{\#1}$	106.6(1)	106.2	106.8
N(2)—Fe(1)—S(1)	106.5(1)	106.1	106.8
N(1)—Fe(1)—S(1)	107.2(1)	109.4	109.7
S(1)$^{\#1}$—Fe(1)—S(1)	105.87(4)	109.6	106.9
N(2)—Fe(1)—Fe(1)$^{\#1}$	121.9(1)	122.0	121.1
N(1)—Fe(1)—Fe(1)$^{\#1}$	118.9(1)	122.0	121.7
S(1)$^{\#1}$—Fe(1)—Fe(1)$^{\#1}$	53.10(4)	54.8	53.5
S(1)—Fe(1)—Fe(1)$^{\#1}$	52.76(4)	54.8	53.4
C(1)—S(1)—Fe(1)$^{\#1}$	111.6(2)	110.1	109.6
C(1)—S(1)—Fe(1)	104.4(1)	110.1	109.2
Fe(1)$^{\#1}$—S(1)—Fe(1)	74.13(4)	70.4	73.0
O(1)—N(1)—Fe(1)	170.3(4)	168.0	169.2
O(2)—N(2)—Fe(1)	169.5(4)	168.0	169.2
C(1)—N(3)—C(2)	114.2(4)	115.8	115.3
N(3)—C(1)—N(5)	128.6(4)	127.4	128.1
N(3)—C(1)—S(1)	119.0(3)	116.2	115.8
N(5)—C(1)—S(1)	112.3(3)	116.2	116.0
C(1)—N(5)—C(4)	114.2(4)	115.8	115.3
N(5)—C(4)—C(3)	123.1(5)	122.3	122.4
C(2)—C(3)—C(4)	116.8(5)	116.3	116.6
N(3)—C(2)—C(3)	123.1(6)	122.4	122.3

$^{\#1}$ $-x, -y, -z + 1$.

6-311++G** basis set was used in the B3LYP method for the calculation of full energies.

The technique of work under a nitrogen atmosphere was described.[7,11]

The amount of NO formed was estimated spectrophotometrically using a known procedure[7] by the amount of formed HbNO.

A homogeneous solution of serum hemoglobin was prepared from the commercial sample (MP Biomedicals) using an earlier described method.[14]

Kinetics of the reaction of Hb with complex 1. A 0.05 *M* phosphate buffer with pH 7.0 (2.8 mL) and a solution of Hb (0.1 mL) to a concentration of $2.26 \cdot 10^{-5}$ mol L^{-1} were introduced into a 4-mL anaerobic experimental cell with the optical path length 1 cm, and the absorption spectrum was recorded. An anaerobic absolute DMSO was added to a weighed sample nitrosyl complex **1** in a vessel filled with nitrogen in such a way that a solution of complex **1** with a concentration of $6 \cdot 10^{-3}$ mol L^{-1} would be obtained. Then the solution was stirred for 3—5 min until complex **1** dissolved completely, and 0.1 mL of the resulting solution was added to the experimental cell with Hb and the same amount was added to the reference cell containing an anaerobic buffer (2.9 mL). The final concentration of nitrosyl complex **1** was $2 \cdot 10^{-4}$ mol L^{-1}, and the DMSO concentration was 3.3%. The differential absorption spectra were recorded: the first spectrum was recorded 0.5 min after the beginning of the reaction, and the subsequent spectra were detected at intervals of 3 min. The spectra were recorded until Hb transformed completely into HbNO, when the spectrum stopped changing.

Experiments on the hydrolysis rate of compound 1 at different pH values (6.0—7.76) were carried out in a nitrogen atmosphere. An anaerobic 0.05 *M* phosphate buffer (pH 6.0, 7.0, or 7.6) (2.9 mL) was introduced into the evacuated 4-mL experimental cell with the optical path length 1 cm. The cell was incubated for 5—10 min at 25 °C. A solution of complex **1** (0.1 mL, $6 \cdot 10^{-3}$ mol L^{-1}) was introduced into the cell with the phosphate buffer with the chosen pH value (6.0—7.76). The final concentration of complex **1** was $2 \cdot 10^{-4}$ mol L^{-1}, and that of DMSO was 3.3%. The absorption spectra were recorded in the visible region (λ = 450—650 nm): the first spectrum was detected 0.5—1 min after the beginning of the reaction, the subsequent spectra were recorded at intervals of 2 min for the first 10 min of the reaction, and then at intervals of 5, 10, 20, and 30 min. The spectra were recorded for 4—5 h.

For the electrochemical determination of the concentration of NO generated by complex **1** in the solutions under study, the amiNO-700 sensor electrode (inNO Nitric Oxide Measuring System, Innovative Instruments, Inc., Tampa, FL, USA) was used. The NO concentration was detected during ~200 s (with an increment of 0.2 s) in a 1% aqueous solution of DMSO containing complex **1** (0.1 μmol L^{-1}). A standard aqueous solution of $NaNO_2$ (100 μmol L^{-1}), which was added to a mixture of aqueous solutions of KI (18 mL, 0.12 mol L^{-1}) and H_2SO_4 (2 mL, 1 mol L^{-1}), was used for the calibration of the electrochemical sensor. The experiments were carried out in anaerobic and aerobic solutions at 25 °C. The pH values of the solutions were measured with an HI 8314 membrane pH-meter (HANNA Instruments, Germany). Buffer solutions were prepared according to an earlier described procedure.[22]

Results and Discussion

Complex **1** was synthesized by the exchange reaction[23] of thiosulfate ligands by heterocyclic ligands (Scheme 1).

Scheme 1

$$[Fe_2(S_2O_3)_2(NO)_4]^{2-} + S_2O_3^{2-} \longrightarrow$$

$$\longrightarrow [Fe(S_2O_3)_2(NO)_2]^{3-} \xrightarrow[-\,2\,S_2O^{2-}]{+\,2\,C_4H_3N_2S^-,\ n\ OH^-}$$

$$\longrightarrow [Fe_2(SC_4H_3N_2)_2(NO)_4]$$

There are several possible modes of coordination of the iron atoms by thiol due to the high coordinating ability of 2-mercaptopyrimidine.[24–27] At low pH values 2-mercaptopyrimidine coordinates to the iron atom through the nitrogen atom of the pyrimidine ring, and with pH increase complexes are predominantly formed in which the ligands are bound to the iron atom through the mercapto group.[28] It was found by the theoretical analysis of the IR spectra that in the solid state $C_4H_3N_2SH$ contains the both forms of the compound (thione and thiol),[29] favoring different coordination modes of the ligand.

According to the X-ray diffraction data, complex **1** (Fig. 1) is formed by two structural units $[Fe(SC_4H_3N_2)(NO)_2]$ connected to each other through the inversion center. The complex is diamagnetic as the earlier obtained pyridine nitrosyl iron complex of the μ_2-S type $[Fe_2(\mu_2\text{-}SC_5H_4N)_2(NO)_4]$ (**2**).[30] The geometry of complex **1** is similar to those for the neutral complexes $[Fe_2(\mu_2\text{-}SR)_2(NO)_4]$ with R = Me, Et, *n*-C_5H_{11}, and Bu^t: the iron atoms coordinated by two NO groups are bound to each other by the bridging sulfur atoms[31,32] and form the centrosymmetric dimer.

In complex **1** the iron atoms have tetrahedral coordination and lie at a distance of 2.727(1) Å, and the sulfur atoms have the pyramidal configuration. The sum of the angles at the S(1) atom is 290.1°. Complex **1** contains no additional coordination of the iron atoms of the pyrimidine cycles (Fe(1)...N(3) 4.77 Å, Fe(1)...N(5) 3.71 Å, Fe(1A)...N(3) 3.46 Å, and Fe(1A)...N(5) 4.54 Å). The Fe(1)—S(1)—C(1)—N(3) torsion angle is 101°. The angle between the Fe(1)S(1)Fe(1A)S(1A) plane and the plane of the C(1)N(5)...N(3) azaheterocycle is 110.1°. For this arrangement of the pyrimidine cycles, the intramolecular N...N contacts between the pyrimidine cycles and nitrosyl groups (N(3)...N(2A) and N(3A)...N(2)) are 2.995 Å.

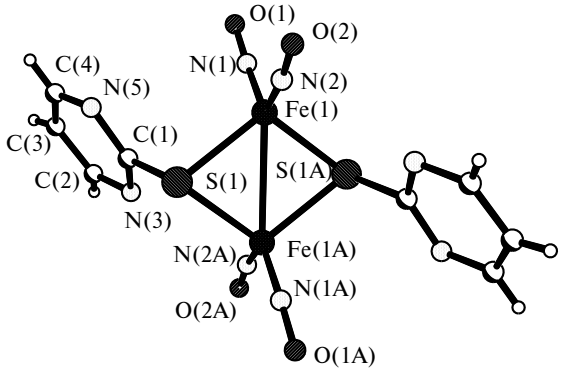

Fig. 1. Molecular structure of complex **1**.

In complex **1** the Fe—S bond lengths (2.267(1) and 2.257(1) Å) are close to those in other complexes of the μ_2-S type: for neutral complex **2** and anionic thiosulfate complexes $[Me_4N]_2Fe_2(\mu\text{-}S_2O_3)_2(NO)_4$ (**3**), $[Bu^n{}_4N]_2Fe_2(\mu\text{-}S_2O_3)_2(NO)_4$ (**4**), and $[Ph_4P]_2Fe_2(\mu\text{-}S_2O_3)_2(NO)_4$ (**5**) they are equal[33–35] to 2.280(1), 2.259(2) 2.251(4) and 2.248(3) Å, respectively. The C—S bond length in complex **1** is 1.800(5) Å, which also coincides with the analogous value for earlier[36] studied neutral complex **2** (1.810(1) Å) and indicates that pyrimidin-2-yl is coordinated by iron in the thiol form.

In the pyrimidine cycle the N(5)—C(1) and N(5)—C(4) (1.331(6) and 1.333(6) Å) bonds are symmetric, whereas the bonds involving the N(3) atom having the shortened contact with the N(2A) nitrogen atom of the nitrosyl group differ slightly (N(3)—C(1) 1.317(6) Å and N(3)—C(2) 1.343(6) Å). The X-ray structure studies of the anionic[33–35] and neutral complexes[34,37,38] indicate a substantial scatter of the bond lengths in the nitrosyl groups. The analysis of the Fe—N—O structural fragments in complex **1** showed that the coordination of the both NO groups is the same within experimental errors. The Fe(1)—N(1) and Fe(1)—N(2) distances are 1.668(4) and 1.663(4) Å, N(1)—O(1) and N(2)—O(2) are 1.170(5) and 1.166(5) Å, respectively, and the Fe—N—O angles are 170.3(4) and 169.5(4)°. Since the pyrimidine cycle is asymmetric as mentioned above, it is unclear why the short intramolecular N...N contacts exert no effect on the coordination of the NO ligands. The observed nonequivalence of the C—C bonds in the pyrimidine cycle (1.356(8) and 1.364(8) Å) is within the statistical error σ.

The DFT calculation of the geometric structure of complex **1** in the isolated state gives the structure with the symmetry C_{2h}.[29] The experimental bond lengths and bond angles are rather well described (Table 3), and the description by the PBE functional is somewhat better than that for the B3LYP functional. The pyrimidine rings are arranged symmetrically relative to the Fe atoms at the intramolecular Fe...N distances 3.58 Å. The Fe(1)—S(1)—C(1)—N(3) torsion angle is 129.8° and differs from the experimental one (110.1°). As a result, the intramolecular contacts between the nitrogen atoms of the pyrimidine and nitrosyl groups increase to 3.16 Å. The energy change upon rotation of the pyrimidine cycles about the C—S bonds is insignificant (<1 kcal mol^{-1}) and, hence, the positions of planes of these cycles is very sensitive to packing effects. At the same time, the analysis of the distribution of the N—C bond lengths in the pyrimidine cycle in the symmetric calculated structure shows that the theoretical C—N bond lengths are the same within 0.005 Å,

which is quite consistent with similarity of the experimental N(5)—C(1) and N(5)—C(4) distances. The C(1)—N(3) bond shortens due the intramolecular N...N contacts and simultaneously the $Fe(NO)_2$ fragments somewhat rotate about the Fe—Fe bonds, which is a reason, most likely, for the same geometric parameters of both NO groups.

The coordination environment of the Fe(1) and Fe(1A) atoms in complex **1** does not differ from the coordination environment of the iron atoms in complex **2**. The ^{57}Fe Mössbauer spectrum of polycrystals **1** looks like a single doublet, which confirms structural equivalence of the iron atoms at room temperature. The spectrum of complex **1** exhibits a slight decrease in the isomeric shift δ_{Fe} (ΔE_Q = 1.264(1) mm s^{-1}, δ_{Fe} = 0.169(2) mm s^{-1}) compared to that for complex **2** (ΔE_Q = 1.262(1) mm s^{-1}, δ_{Fe} = 0.177(2) mm s^{-1}) at the almost constant quadrupole splitting ΔE_Q. This indicates an increase in the 4s-electron density on the iron atom in complex **1** and agrees with the shortening of the Fe—S bond (2.262(1) Å) compared to that in complex **2** (2.280(1) Å). A correlation between the positions of the absorption bands of vibrations of the NO groups in the IR spectra (1748, 1797 cm^{-1} for complex **1** and 1734, 1792 cm^{-1} for complex **2**) with the isomeric shift values is observed: a decrease in the isomeric shift is accompanied by an increase in the frequencies of stretching vibrations of the NO groups.

One binuclear structural unit falls on a unit cell in complex **1**. The crystal structure is formed by the multiplication of this structural unit by translations along the unit cell axes. The projection of crystal structure **1** is shown in Fig. 2. In crystal **1** the binuclear complexes are bound to each other by van der Waals interactions. The structure contains shorten contacts between the NO ligands in piles along the direction of the *a* axis (N(1)...O(2) 2.984 Å) and between the carbon atoms of the pyrimidine ligands of the adjacent piles arranged in the direction of the diagonal (0 −1 1) (C(3)...C(3) 3.384 Å).

On storage in light without moisture complex **1** is less stable than complex **2**. When complex **1** is stored under conditions of elevated moisture content, the complex decomposes appreciably accompanied by the change in color and crystallinity. The complex is well soluble in CH_2Cl_2, $CHCl_3$, and CCl_4, its solubility is lower in THF and DMSO, whereas in acetone and dimethyl ether the complex decomposes instantly.

Several approaches were used to study the kinetics of formation of NO generated by complex **1** in aqueous solutions. It is known,[39,40] Hb reacts with the first NO molecule with a rate constant of 1.02 • 10^8 L mol^{-1} s^{-1}, which is close to the diffusion-controlled value, and has very high constant of NO binding: 3 • 10^{10} L mol^{-1}. According to literature data, the subsequent NO molecule add to other heme complexes of Hb with the same rate (or more rapidly). Therefore, in the presence of the NO donor, NO molecules that appear in the solution almost irreversibly

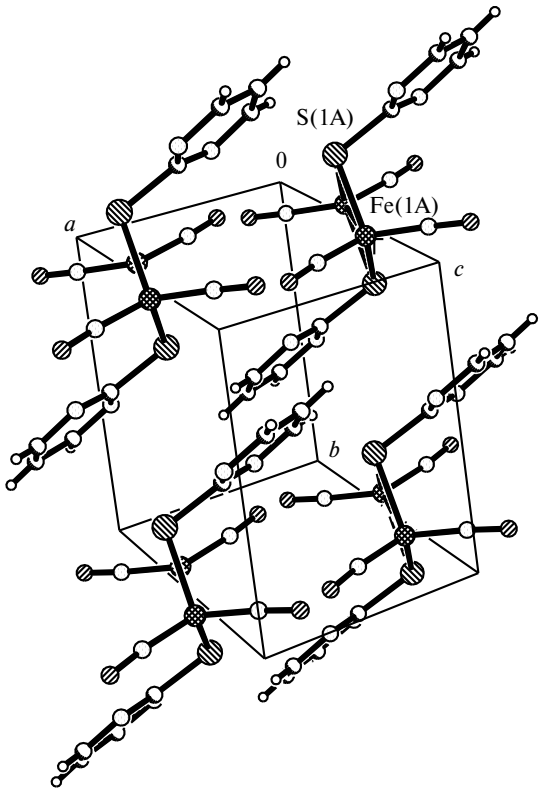

Fig. 2. Projection of crystal structure **1**.

bind with Hb until free centers for NO coordination disappear. For simplicity of analysis we consider that the formation of any heme complex of NO in the system occurs independently and the respective equilibrium constants are equal for binding of each of the four NO molecules. This case is described by Scheme 2.

Scheme 2

$$LFe(NO) \xrightarrow{k_1} LFe + NO$$

$$Fe^{Hb} + NO \underset{}{\overset{K}{\rightleftharpoons}} Fe^{Hb}(NO)$$

$L = [Fe(\mu_2\text{-}SC_4H_3N_2)_2(NO)_3]$

Here Fe^{Hb} is one of four heme centers of Hb, and its concentration in any moment *t* satisfies the condition

$$x(t) = K[a - x(t)]\{b[1 - \exp(-k_1 t)] - x(t)\},$$

where $a = 4[Hb]_0$ and $b = [LFe(NO)]_0$. The kinetic dependence $x(t)$ can easily be expressed in the analytical form but can also be approximated conveniently by the effective kinetic curve of the first order[7]

$$x(t) \approx \tilde{b}[1 - \exp(-\tilde{k}_1 t)].$$

The fitting constants $b\sim$ and $k\sim_1$ are chosen on the basis of the condition of the best of experimental data description. However, the $b\sim$ value can differ from the $[LFe(NO)]_0$ value. At the same time, the initial linear region of the $x(t)$ curve with allowance for the high value of equilibrium constant K is determined only by the product

$$bk_1x(t) \sim Kabk_1t/(1 + Ka) \sim bk_1t.$$

Therefore, the following ratio should be fulfilled: $\widetilde{b}\widetilde{k}_1 \approx bk_1$.

The kinetics of changing the differential absorption spectra in time upon the interaction of complex **1** with Hb at neutral pH is shown in Fig. 3. The absorption decreases at 565 nm and increases in the region 450—540 nm and at 575 nm, indicating the formation of HbNO. The data on the kinetics of HbNO formation in the presence of complex **1** were obtained from the analysis of these spectra (Fig. 4). As for the earlier studied compounds,[7,11] they are well described in terms of the formalism of pseudo-first order reactions, which for the rate constant of NO evolution gives a value of $3.7 \cdot 10^{-4}$ s^{-1}. The close value ($3.5 \cdot 10^{-4}$ s^{-1}) was obtained when the whole kinetic curve was processed in the framework of full Scheme 2.

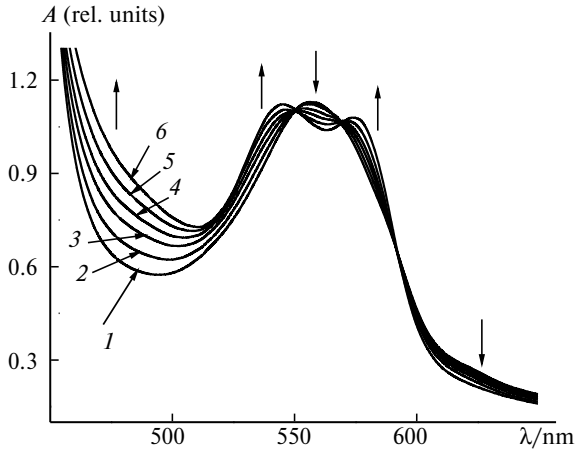

Fig. 3. Kinetics of changes in the differential absorption spectra upon the reaction of complex **1** ($2 \cdot 10^{-4}$ mol L^{-1}) with Hb ($2.26 \cdot 10^{-5}$ mol L^{-1}). The spectra were recorded 0.8 (*1*), 6 (*2*), 17 (*3*), 29 (*4*), 46 (*5*), and 85 min (*6*) after the beginning of the reaction.

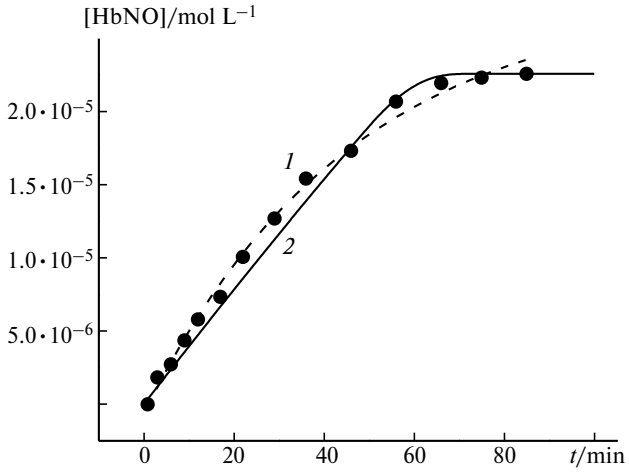

Fig. 4. Kinetics of HbNO formation by the reaction of complex **1** ($2 \cdot 10^{-4}$ mol L^{-1}) with Hb ($2.26 \cdot 10^{-5}$ mol L^{-1}) according to the results of spectral studies (see Fig. 3). Points are experiment, and the theoretical curves are plotted on the basis of the pseudo-first-order kinetics (*1*) and in terms of full Scheme 2 (*2*).

The dependence of the hydrolysis rate of complex **1** on the pH of the medium was also studied by the detection of changes in the absorption spectra of complex **1** in aqueous buffer solutions in the pH interval from 6.0 to 7.76 (Fig. 5). The measured absorbance values A at the wavelength 450 nm was processed according to the kinetics of the first-order reaction approximating then by the equation

$$A = A_\infty + (A_\infty - A_0)\exp(-k_2t).$$

The obtained k_2 values are listed in Table 4. The dependence of k_2 on pH has a pronounced extreme character. The spectra change most slowly in a neutral medium, and hydrolysis is strongly accelerated with an increase or decrease in the pH. As can be seen from the data in Table 4. the rate constants for NO evolution k_2 at pH 7 and the constant k_1 ($3.7 \cdot 10^{-4}$ s^{-1}), which was also determined by the data on the reaction with Hb (see Fig. 3, differ noticeably.

To analyze and interpret these data, first let us consider the results of direct anaerobic measurements of the NO concentration during hydrolysis of complex **1** by the electrochemical method. The kinetic changes in the amount of NO evolved to solution at different pH values under the same conditions but in the absence of Hb are shown in Fig. 6. These kinetic dependences are qualitatively different because of the maximum, whose appearance can be due to the subsequent transformation of NO. Simplest two-stage Scheme 3 was used for the description of these dependences. Scheme 3 gives the following functional time dependence of the NO concentration:

$$[NO] = ck_3[\exp(-k_4t) - \exp(-k_3t)]/(k_3 - k_4).$$

Table 4. Kinetic parameters (k/s^{-1}) obtained by the spectrophotometric (I) and electrochemical (II) methods for complex **1** ($2 \cdot 10^{-4}$ mol L^{-1}) at pH 6.0—7.76 and 25 °C

pH	I, k_2	II		
		c^a	$k_3{}^b$	k_4
6.0	$(4.2\pm0.2) \cdot 10^{-4}$	0.853	0.0146 (0.0147)	$4.29 \cdot 10^{-4}$
7.0	$(9.7\pm0.5) \cdot 10^{-5}$	0.0983	0.00796 (0.00897)	$\sim 1 \cdot 10^{-7}$
7.43	—	0.249	0.0213 (0.0209)	$8.16 \cdot 10^{-4}$
7.76	$(2.5\pm0.15) \cdot 10^{-4}$	—	(0.0439)	—

[a] Number of moles of [NO] per mole of the complex.
[b] The result of calculation by Scheme 3 is given in parentheses.

Scheme 3

$$LFe(NO) \xrightarrow{k_3} LFe + NO$$

$$NO \xrightarrow{k_4} P$$

L = $[Fe(\mu_2\text{-}SC_4H_3N_2)_2(NO)_3]$, P — продукты

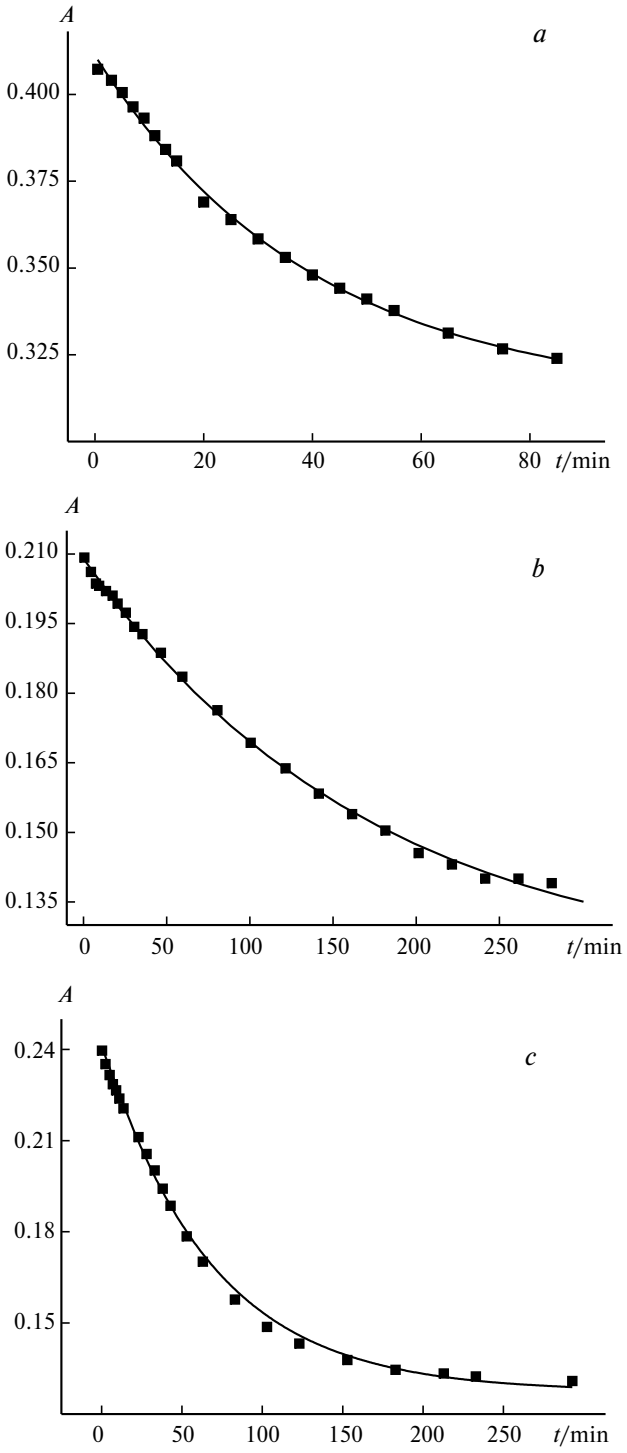

Fig. 5. Kinetic curves of hydrolysis of complex **1** at pH 6.0 (*a*), 7.0 (*b*), and 7.76 (*c*); the *A* values are given for λ = 450 nm.

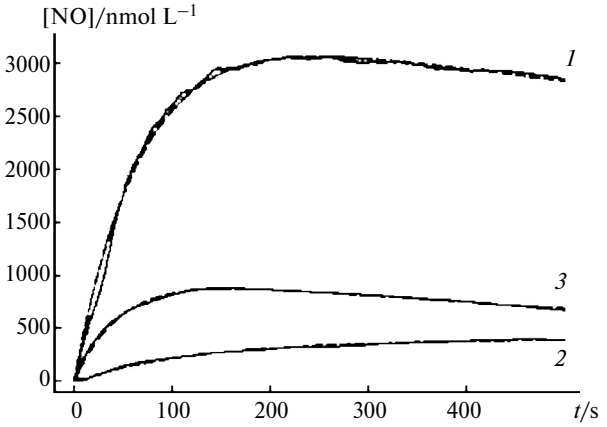

Fig. 6. Time dependences of the NO concentration for the decomposition of complex **1** ($4 \cdot 10^{-6}$ mol L^{-1}) under anaerobic conditions at 25 °C for different pH values of aqueous solutions: pH = 6.0 (*1*), 7.0 (*2*), and 7.43 (*3*). Dashed lines are the result of approximation of the kinetic curves.

The c, k_3, and k_4 values determined by the experimental data using the least-squares method are given in Table 4. It should be mentioned that the accuracy of determination of the rate constant k_4 in a neutral medium is low, because the kinetic curve has no maximum before 500 s. The physical sense of the c constant is the limiting concentration of NO, which would be observed in the absence of further NO transformation. Note that the limiting amount of NO molecules that fall on one iron-nitrosyl complex is smaller than the minimum stoichiometric amount equal to unity. What factors can result in this process?

Let us consider the nature of possible reactions leading to the disappearance of NO in the system. Based on observations of the formation of nitrous oxide in solutions of dinitrosyl iron complexes,[41,42] we believe that the final product of NO transformation is N_2O. The formation of nitrous oxide indicates the formation of the N—N bond. Two NO molecules give no strong binding between each other, and an NO molecule in the reduced form is required for strong binding. As it is known, NO and NO^- interact with the high rate[43] affording the $ONNO^-$ hyponitrite radical anion with strong oxidative properties.[44] Nitrous oxide is formed by its further transformations. Two HNO nitroxyls (protonated form of NO^-) are dimerized to form an unstable HONNOH molecule decomposing to N_2O and H_2O. However, the protonation of NO^- is a spin-forbidden reaction and, hence, the interaction of NO and NO^- can be considered as the most probable elementary step leading to nitrous oxide.

A reducing agent is needed to form NO^- from NO. The standard redox potential of NO is $-0.8(\pm0.2)$ V.[45] We believe that complex **1** acts as such a reducing agent after the dissociation of the Fe—NO bond and coordination of a solvent molecule (water) to the free coordination site. The enhancement of its reduction properties compared to

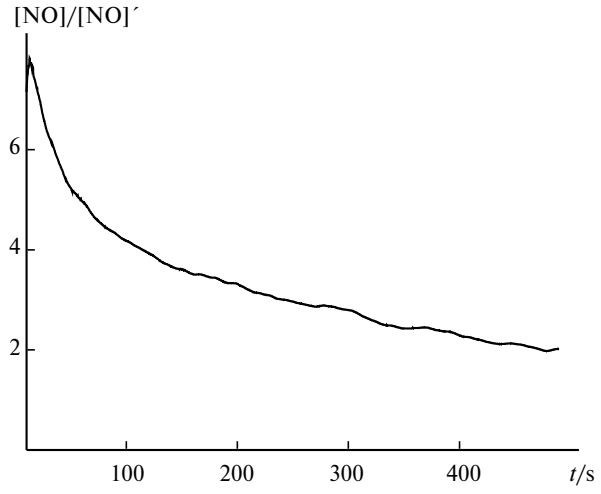

Fig. 7. Time dependence of the ratio of NO concentrations under aerobic and anaerobic conditions ([NO] and [NO]´, respectively) in an aqueous solution during the decomposition of complex **1** ($4 \cdot 10^{-6}$ mol L^{-1}) at pH 6.0 and 25 °C.

the starting complex is a consequence of an increase in the electron density on the Fe atom due to the coordination of the donating water molecule. This point of view is indirectly confirmed by the increase by several times in the amount of NO evolved under anaerobic conditions.

The data on the amount of NO evolved in an aqueous solution of complex **1** under aerobic and anaerobic conditions in the same medium are presented in Fig. 7. As can be seen from the data in Fig. 7, the amount of NO evolved under aerobic conditions is larger at the initial stages of the process. This can be explained by the faster electron transfer to the oxygen molecule from the reduced complex. As known, O_2^- also possess the reduction properties and the standard redox potential of O_2/O_2^- is similar: −0.61 V. As a result of this competitive redox process, the fraction of reduced NO molecules, which disappear in the subsequent reactions, decreases and the observed NO concentration thus increases.

The direct interaction of NO from the solution with the negatively charged NO ligand (Table 5) of the nitrosyl iron complex is a route alternative to the outer-sphere electron transfer to NO. This route affords the hyponitrite ligand in the coordination sphere. In this process an electron is also transferred in fact to the NO molecule but without the escape of the latter from the coordination sphere. This is the route that is proposed as an elementary step of NO reduction of nitrous oxide and water involving the binuclear iron complexes in the active center of flavoprotein of the A type from *Moorella thermoacetica*.[46] It is quite evident that when this mechanism occurs in the case of rather fast reactions of hyponitrite ligand formation, its

Table 5. Electronic characteristics[a] of complexes $[Fe_2(\mu\text{-}SC_4H_3N_n)_2(NO)_2]$

Complex	E_{rel} /kcal mol^{-1}	Fe		NO		S		$<S^2>$	$<S^2>^b$
		I	II	I	II	I	II		
Calculation by B3LYP/6-31G* method									
1	0 [c]	0.61	−2.41	−0.21	0.85	−0.15	0.00	2.60	10.72
			2.41		−0.85				
6a	10.1	0.87	−3.20	−0.26	1.20, 1.16	−0.30	−0.03	4.56	15.05
		0.77	3.26	−0.36	−1.37				
6b	13.6	0.85	3.21	−0.25	−1.19, 1.18	−0.29	0.06	3.93	12.54
			1.52	−0.40	−1.42				
	0	0.85	−3.20	−0.26	1.20, 1.19	−0.29	−0.04	4.66	15.39
		0.87	3.28	−0.40	−1.40				
7	26.1	0.88	3.23	−0.25	−1.19, −1.17	−0.33	0.03	4.19	13.59
		0.65	1.33	−0.33	−1.26				
	0	0.85	−3.22	−0.26	1.17, 1.20	−0.36	−0.03	4.57	15.08
		0.78	3.27	−0.36	−1.37				
Calculation by PBE/SBK method									
1		0.50	—	−0.21	—	−0.03	—	—	—
6a	7.4	0.54	−1.16	−0.24	0.32, 0.34	−0.12	−0.03	—	—
		0.69	2.09	−0.40	−0.49				
6b	0	0.63	1.19	−0.30	−0.36, −0.36	−0.13	0.05	—	—
		0.68	0.46	−0.49	−0.1				
7		0.51	−1.09	−0.25	0.30, 0.31	−0.13	−0.04	—	—
		0.76	2.06	−0.41	−0.52				

[a] I is charge, and II is spin density.

[b] Average value of the squared spin after the annihilation of the component of the wave function having spins 1 and 3/2 for the singlet and doublet, respectively.

[c] Characteristics of the singlet state with violated symmetry.

description in terms of Scheme 3 would decrease c (the limiting amount of NO molecules). In addition, this simple kinetic scheme ignores that the disappearance of NO due to the formation of the hyponitrite radical anion $ONNO^-$ is in fact the reaction of the second order with respect to [NO]. Therefore, its probability increases with the decomposition of the complex, which can be described only due to a decrease in the effective limiting amount of NO molecules formed upon the decomposition of one complex, if the kinetics of NO consumption is approximated by the effective first-order law. It is also clear that protolytic equilibria can result in charged forms of the nitrosyl iron complexes with changed physicochemical properties, which changes the ratio of two routes of NO transformation. Therefore, it is not surprising that the c parameter (see Scheme 3) depends on pH. The reasons for which this dependence, as well as the dependences of k_1 and k_2 on pH, is also extreme seem unclear, and additional studies are needed to elucidate them. Nevertheless, assuming the key participation of a proton or a hydroxyl ion during Fe—NO bond dissociation, one can formally describe the influence of pH by the introduction of partial rate constants of the second order for the decomposition of the complex and NO transformation by the action of $[H^+]$ or $[OH^-]$

$$k_3 = k_{3H}[H^+] + k_{3OH}[OH^-],$$

$k_{3H} = 2.72 \cdot 10^4$ L mol^{-1} s^{-1}, $k_{3OH} = 2.54 \cdot 10^4$ L mol^{-1} s^{-1}.

The k_4 constant can be presented analogously

$$k_4 = k_{4H}[H^+] + k_{4OH}[OH^-],$$

$k_{4H} = 1.36 \cdot 10^4$ L mol^{-1} s^{-1}, $k_{4OH} = 7.58 \cdot 10^4$ L mol^{-1} s^{-1}.

This formal representation makes it possible to describe (with good accuracy) the measured dependences of the NO generation rate on pH (see the values in the parentheses in Table 4). The calculation shows that minimum k_3 value is achieved in a neutral medium, and k_4 is 0.0064 s^{-1} at pH 6.63.

For neutral media we can compare the rate constant for the appearance of NO in solution (k_3) measured by the electrochemical method and the rate constant of dinitrosyl complex dissociation (k_1) in the system with Hb (see Table 4). It is seen that they differ by an order of magnitude. The reason for this inconsistency can be as follows. As we have shown previously,[11] not only NO molecules and the nitrosyl iron complexes themselves can bind to Hb. As a result, their NO-donor ability can change. However, to explain such a high value of the effect, it should be accepted that one protein globule of Hb can bind ~10 molecules of complex **1**. Further studied are required to reveal the exact reason for this inconsistency. Anyway, the data obtained indicate that the chemistry and mechanism of decomposition of the nitrosyl iron complex under study changes in the presence of Hb.

The study of spectral changes upon hydrolysis in the absence of Hb (see Fig. 5) shows that the dependence of their rate on pH is also extreme (see Table 4). The change in the molar absorption coefficient of the initial solution of complex **1** at the wavelength 450 nm is also extreme, which indirectly indicates the changes in its state in both acidic and alkaline media. However, spectral changes in the absence of Hb are also much slower (rate constant $k_2 = (9.7 \pm 0.5) \cdot 10^{-5}$ s^{-1}) than NO accumulation in solution at pH 7 (rate constant $k_3 = 7.96 \cdot 10^{-3}$ s^{-1}). Moreover, according to the data obtained, the accumulation of nitrosylated Hb in neutral media is threefold faster than the spectral changes at the wavelength 450 nm.

To reveal reasons for these distinctions, let us deconvolute the absorption spectrum in the region 450—653 nm to linearly independent components during the decomposition of the complex at pH 7.0. It turned out that the whole spectrum is described with good accuracy at an arbitrary moment by a linear combination of only two components. Since the k_2 and k_4 values are close and taking into account the data obtained on the deconvolution of the spectra to the components, we can propose the following explanation of the inconsistency. We suppose that the spectrum of complex **1** at 450—650 nm remains almost unchanged during Fe—NO bond dissociation and all changes occur only upon its subsequent reactions with NO molecules in solution. Since this is accompanied, according to our concepts, by a change in the charge state of the complex, it seems reasonable to expect greater changes in the absorption spectrum of the complex.

Unlike the earlier studied nitrosyl iron complexes of the μ-N—C—S type,[7] the rate of decomposition of complex **1** is lower by an order of magnitude. Thus, the generation of NO to solution by the studied complex of the μ_2-S type, as well as by complex **2**,[11] is more prolong. According to accepted concepts, in the related complexes of the μ_2-S type (ethers of Roussin´s red salt $[Fe_2(\mu_2\text{-}SR)_2(NO)_4]$ (R = Alk) the Fe—S bond is cleaved due to the attack of nucleophilic particles and mononuclear paramagnetic species are formed in the solution.[47] For instance, the mononuclear complexes are formed in the presence of an excess of thiolate anions

$$[Fe_2(\mu_2\text{-}SR)_2(NO)_4] + 2\ R'S^- \rightleftharpoons$$

$$\rightleftharpoons 2\ [Fe(SR)(SR')(NO)_2]^-.$$

After the [2Fe—2S] cycle disclosure the both RS^- ligands are rapidly substituted for the acido ligands to form monosubstituted intermediates $[Fe(SR)X(NO)_2]^-$, which are further transformed into disubstituted anions $[Fe(X)_2(NO)_2]^-$ (X = Br^-, I^-, SCN^-, N_3^-, NCO^-, NO_2^-).[48,49] However, in the absence of thiolate anions, "ethers of Roussin´s red salt" are quite stable in alkaline media, most likely, due to the lower nucleophilicity of

OH^- compared to RS^-. In acidic and neutral aqueous solutions the $[Fe_2(\mu_2\text{-}SAlk)_2(NO)_4]$ complexes are also stable and generate no NO. It is known[50] that a strong reducing agent or photoactivation is required for the generation of NO in solutions of these compounds.

The energies of Fe—NO bond dissociation and NO substitution for the aqua ligand in complex **1** were studied by quantum chemical simulation using the DFT methods. The doublet state of the system was considered for the complexes with three NO groups, because the additional calculations showed that the quartet state was higher-lying. The doublet state appears due to the antiparallel orientation of spin 1 of the Fe(NO) node and spin 1/2 of the $Fe(NO)_2$ node (see Table 5). The optimization of binuclear complex **1** by NO ligand removal gave structures **6a**,**b** (Fig. 8). Their specific feature is the formation of additional coordination bonds at the Fe atom with one NO ligand with the nitrogen atoms of the pyrimidine cycles. As a result, the coordination number increases to 4 (for **6a**) or 5 (for **6b**), and the coordination polyhedron becomes a distorted tetrahedron or trigonal bipyramid, respectively. When the coordination number increases from 4 to 5, the energy gain is 7.8 kcal mol^{-1}. Thus, it can be evaluated that the effects of intramolecular stabilization of the intermediate tricoordinated state of the Fe complex after Fe—NO bond dissociation result in an overall energy gain of ~15 kcal mol^{-1}. Naturally, these effects decrease energy expenses to the removal of the nitrosyl ligand, which qualitatively explained the low stability of complex **1**.

However, the calculation of the N—O bond energy meets certain difficulties. A dissociation energy of 29.2 kcal mol^{-1} was obtained by the theoretical B3LYP study[51] of the decomposition of the mononuclear dinitrosyl iron complex (in this case, the tricoordinated state is observed for the product (mononitrosyl iron complex). Based on this value and taking into account the effects of intramolecular stabilization in complex **1**, one could expect a decrease in the N—O bond energy to 14 kcal mol^{-1}. It follows from the comparison of the local spins and the average value of the squared spin for the starting complex **1** and denitrosylated products **6a** and **6b** (see Table 5) that the solution with violated symmetry found for complex **1** has no necessary spin structure, although it is internally stable. It can easily be shown that for the one-determinant function containing n_a unpaired electrons with spin α and n_b unpaired electrons with spin β the average squared spin is as follows:

$$\langle S^2 \rangle = (n_a + n_b)/2 + (n_a - n_b)^2/4.$$

For the initial complex $n_a = n_b = 5$, and after one NO groups was removed $n_b = 4$. Thus, one should expect the values $\langle S^2 \rangle = 5$ and 4.75 for **1** and **6a**,**b**, respectively. The former is poorly consistent with the calculated data (2.60), whereas the second value agrees quite satisfactorily with

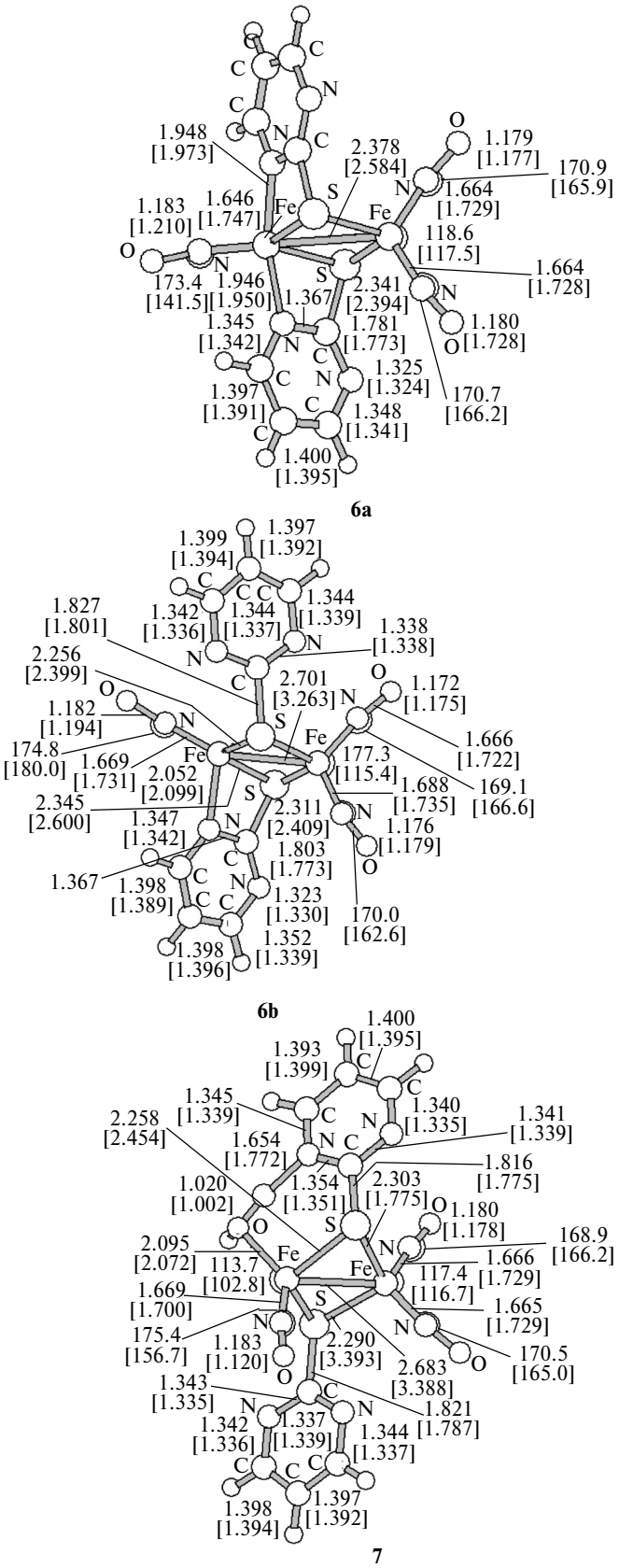

Fig. 8. Structures of binuclear intermediate complexes **6a,b** and **7** for the dissociation of the Fe—NO bond calculated by the B3LYP and PBE methods (in brackets); angles are given in deg and bond lengths are in Å.

4.56 and 4.67. For structures **6a**,**b** we also found the solutions corresponding to the low-spin state of the Fe atom with one NO ligand. In this case, the energy of the system increases by 11 kcal mol^{-1} and $<S^2>$ decreases to 3.93, which agrees with a simple estimate of 3.75 for a decrease in the number of unpaired electrons on one Fe atom (this gives $n_a = 4$, $n_b = 3$). This analysis shows why the calculated energy of the decomposition of the complex (energy gain 10 kcal mol^{-1}) differs noticeably from the above presented estimate: the energy loss if 14 kcal mol^{-1}.

When NO is substituted for a water molecule, complex **7** with the intramolecular hydrogen bond is formed (see Fig. 8). The both Fe atoms have the coordination number 4. The energy bond in H_2O is insignificant: 3 kcal mol^{-1}, because two new coordination Fe—N bonds are formed upon the dissociation of the Fe—O bond. The calculation of the bond energy in a water molecule by the PBE calculation also give the value close to zero.

Thus, based on the calculation performed, we may expect that the direct substitution of the nitrosyl ligand for the aqua ligand in complex **1** would be improbable. This agrees qualitatively with the highest stability of the complex. The increase in the coordination number of the Fe atom to 5 creates prerequisites for studying the associative mechanism of NO substitution for a water molecule. However, it was found that the reaction of complex **1** with H_2O affords only an outer-sphere complex with an energy gain of 5.4 kcal mol^{-1}. The complex simultaneously contains weak hydrogen bonds with the nitrogen atom of the pyrimidine cycle and bridging sulfur atom. At the same time, it is established that the hydroxyl ion can coordinate to the Fe atom. The energy change in this process needs special studies because of high solvation effects. Nevertheless, the decrease in the binding energy of the NO ligand with the pentacoordinated Fe atom in the complex with the hydroxyl ion can be expected. At the same time, the detected formation of a hydrogen bond between the bridging S atom and water molecule indicates that this atom can be protonated. In this case, one can expect the electrophilic assistance for the nucleophilic attack to the Fe atom resulting finally in dissociation to two mononuclear complexes. The facts presented indicate a possible role of the pH influence on the decomposition rate of complex **1**.

The more vigorous generation of NO in an acidic medium compared to an alkaline medium (see Fig. 6) indicates higher efficiency of the electrophilic attack (attack of the proton) compared to the nucleophilic attack of the hydroxyl ion. It is most likely that the hydrolysis of complex **1** at pH ≤ 7 proceeds similarly to that of the dianion of Roussin´s red salt" $[Fe_2(\mu_2\text{-}S)_2(NO)_4]^{2-}$ (**8**). In the latter, the bridging sulfur atoms have higher negative charge: −0.43 (see Ref. 50) or −0.70 (calculated[52] by the B3LYP/6-31G* method). Therefore, the faster decomposition of compound **8** in an acidic medium should be expected. However, in neutral and acidic media "Roussin´s red salt" evolves a smaller amount of NO based on 1 mole of the complex[7] than complex **1**. This is due to the formation of stable polynuclear cluster anions $[Fe_4(\mu_3\text{-}S)_3(NO)_7]^-$, $[Fe_5(\mu_3\text{-}S)_4(NO)_8]^-$, or $[Fe_7(\mu_3\text{-}S)_6(NO)_{10}]^-$, which are formed, in turn, as a result of the aggregation of the protonated intermediates $[Fe_2(\mu_2\text{-}S)(\mu_2\text{-}SH)(NO)_4]^-$ and $[Fe_2(\mu_2\text{-}SH)_2(NO)_4]^-$ primarily formed during hydrolysis.[53—55] In an alkaline medium the "red salt" is stable and no NO generation occurs (unlike studied complex **1**), which can reasonably be related to its resistance to the nucleophilic attack due to the high negative charge.

The theoretical study performed shows that the observed effect of pH can be explained by the dissociation of the complex to two mononuclear complexes in an acidic medium by the electrophilic attack of the proton to the S atom and by the associative mechanism of NO substitution for the hydroxyl ion in an alkaline medium. More detailed consideration of the problem along with analysis of other variants is beyond the scope of the present work.

The calculated IR spectra of the binuclear complexes with three NO groups have an interesting feature: the frequency of the stretching vibration of the single NO ligand only slightly (by 10—15 cm^{-1}) differs from the frequency of the antisymmetric stretching vibration of the pair of the NO ligands at another center, but the corresponding band is threefold higher in intensity. As known, the peaks of N—O vibrations are very intense in the spectra of the dinitrosyl iron complexes and, in several cases,[39,51] a small satellite peak appears in the region of doublet of N—O vibrations. This satellite cannot be due to very small amounts of an admixture of the decomposition products with NO elimination because of the specific feature mentioned. Since this admixture is paramagnetic, its presence can violate the run of the magnetic susceptibility of the sample at low temperatures.

Thus, when studying the chemical properties and reactivity of the compounds of the studied class and for the prediction of the NO-donor ability and choice of the functional sulfur-containing ligand, it is important to study their relation to the charge state of the bridging sulfur atoms and atoms of the {Fe—NO} fragment.

The authors are grateful to A. I. Kazakov and A. V. Chudinov for help in the work.

This work was financially supported by the Presidium of the Russian Academy of Sciences (Program No. 15 "Fundamental Sciences for Medicine"), the Russian Foundation for Basic Research (Project No. 06-03-32381), and the Division of Chemistry and Materials Science (Program No. 1 "Theoretical and Experimental Investigation of the Chemical Bond Nature and Mechanisms of the Most Important Chemical Reactions and Processes").

References

1. J. A. McCleverty, *Chem. Rev.*, 2004, **104**, 403; P. C. Ford, L. E. Laverman, *Coord. Chem. Rev.*, 2005, **249**, 391.
2. N. M. Crawford, *J. Experim. Botany*, 2006, **57**, 3.
3. K. M. Davies, D. A. Wink, J. E. Saavedra, L. Keefer, *J. Am. Chem. Soc.*, 2001, **123**, 5473.
4. R. Butler, I. L. Megson, *Chem. Rev.*, 2002, **102**, 1155.
5. A. S. Dutton, J. M. Fukuto, K. N. Houk, *Inorg. Chem.*, 2004, **43**, 1039.
6. A. S. Dutton, Ch. P. Suhrada, K. M. Miranda, D. A. Wink, J. M. Fukuto, K. N. Houk, *Inorg. Chem.*, 2006, **45**, 2448.
7. N. A. Sanina, L. A. Syrtsova, N. I. Shkondina, T. N. Rudneva, E. S. Malkova, T. A. Bazanov, A. I. Kotel'nikov, S. M. Aldoshin, *Nitric Oxide: Biol. Chem.*, 2007, **16**, 181.
8. O. S. Zhukova, N. A. Sanina, L. V. Fetisova, G. K. Gerasimova, *Ros. Bioterapevt. Zh.* [*Russian Biotherapeutical Journal*], 2006, **5**, 14 (in Russian).
9. A. A. Timoshin, A. F. Vanin, Ts. R. Orlova, N. A. Sanina, E. K. Ruuge, S. M. Aldoshin, E. I. Chazov, *Nitric Oxide: Biol. Chem.*, 2007, **16**, 286.
10. L. M. Borisova, I. Yu. Kubasova, M. P. Kiseleva, Z. S. Smirnova, N. A. Sanina, S. M. Aldoshin, T. N. Rudneva, *Ros. Bioterapevt. Zh.* [*Russian Biotherapeutical Journal*], 2007, **6**, 42 (in Russian).
11. N. A. Sanina, L. A. Syrtsova, N. I. Shkondina, E. S. Malkova, A. I. Kotel´nikov, S. M. Aldoshin, *Izv. Akad. Nauk*, *Ser. Khim.*, 2007, 732 [*Russ. Chem. Bull., Int. Ed.*, 2007, **56**, 761].
12. D. A. Wink, J. B. Mitchell, *Free Radical Biol. Med.*, 1998, **25**, 434.
13. J. A. Montgomery, *Medicinal Research Revs*, 1982, **2**, 271.
14. A. Amici, M. Emanuelli, G. Magni, N. Raffaelli, S. Ruggieri, *FEBS Lett.*, 1997, **419**, 263.
15. S. Raic-Malic, D. Svedruzic, T. Gazivoda, A. Marunovic, A. Hergold-Brundic, A. Nagl, J. Balzarini, E. De Clercq, M. Mintas, *J. Med. Chem.*, 2000, **43**, 4806.
16. *Khimioterapiya opukholevykh zabolevanii* [*Chemotherapy of Tumor Diseases*], Ed. N. N. Blokhin, Meditsina, Moscow, 1984 (in Russian).
17. N. A. Sanina, S. M. Aldoshin, T. N. Rudneva, N. I. Golovina, G. V. Shilov, Yu. M. Shul´ga, V. M. Martynenko, N. S. Ovanesyan, *Koord. Khim.*, 2005, **31**, 323 [*Coord. Chem.* (*Engl. Transl.*), 2005, **31**].
18. A. Weissberger, E. Proskauer, J. A. Riddick, E. E. Toops, *Organic Solvents: Physical Properties and Methods of Purification*, Wiley, New York, 1955.
19. V. A. Klimova, *Osnovnye mikrometody analiza organicheskikh soedinenii* [*Main Micromethods of Analysis of Organic Compounds*], Khimiya, Moscow, 1975, 21 (in Russian).
20. G. M. Sheldrick, *SHELX-97, Release 97-2. Program of Crystal Structure Refinement*, University of Göttingen, Göttingen, Germany, 1997.
21. M. J. Frisch, G. W. Trucks, H. B. Schlegel, G. E. Scuseria, M. A. Robb, J. R. Cheeseman, V. G. Zakrzewski, J. A. Montgomery, Jr., R. E. Stratmann, J. C. Burant, S. Dapprich, J. M. Millam, A. D. Daniels, K. N. Kudin, M. C. Strain, O. Farkas, J. Tomasi, V. Barone, M. Cossi, R. Cammi, B. Mennucci, C. Pomelli, C. Adamo, S. Clifford, J. Ochterski, G. A. Petersson, P. Y. Ayala, Q. Cui, K. Morokuma, D. K. Malick, A. D. Rabuck, K. Raghavachari, J. B. Foresman, J. Cioslowski, J. V. Ortiz, A. G. Baboul, B. B. Stefanov, G. Liu, A. Liashenko, P. Piskorz, I. Komaromi, R. Gomperts, R. L. Martin, D. J. Fox, T. Keith, M. A. Al-Laham, C. Y. Peng, A. Nanayakkara, C. Gonzalez, M. Challacombe, P. M. W. Gill, B. Johnson, W. Chen, M. W. Wong, J. L. Andres, C. Gonzalez, M. Head-Gordon, E. S. Replogle, J. A. Pople, *GAUSSIAN-98, Revision A.7*, Gaussian, Inc., Pittsburgh (PA), 1998.
22. *Kratkii spravochnik khimika* [*Brief Chemist´s Manual*], Ed. B. I. Perel´man, Moscow, Khimiya, 1963, 467 (in Russian).
23. N. A. Sanina, T. N. Rudneva, S. M. Aldoshin, G. V. Shilov, D. V. Korchagin, Yu. M. Shul´ga, V. M. Martinenko, N. S. Ovanesyan, *Inorg. Chim. Acta*, 2006, **359**, 570.
24. S. G. Rosenfield, P. K. Mascharak, S. K. Arora, *Inorg. Chim. Acta*, 1987, **129**, 39.
25. M. E. Lizarraga, R. Navarro, E. P. Urriolabeitia, *J. Organometal. Chem.* 1997, **542**, 51.
26. J. Jolley, W. I. Cross, R. G. Pritchard, C. A. McAuliffe, K. B. Nolan, *Inorg. Chim. Acta*, 2001, **315**, 36.
27. I. A. Lathan, G. J. Leigh, Ch. J. Pickett, G. Huttner, I. Jibrill, J. Zubieta, *J. Chem. Soc., Dalton Trans.*, 1986, 1181.
28. K. A. Mitchell, C. M. Jensen, *Inorg. Chim. Acta*, 1997, **265**, 103.
29. A. F. Shestakov, Yu. N. Shul´ga, N. S. Emel´yanova, N. A. Sanina, S. M. Aldoshin, *Izv. Akad. Nauk*, *Ser. Khim.*, 2006, 2053 [*Russ. Chem. Bull., Int. Ed.*, 2006, **55**, 2133].
30. O. A. Rakova, N. A. Sanina, G. V. Shilov, Yu. M. Shul´ga, V. M. Martynenko, N. S. Ovanesyan, S. M. Aldoshin, *Koord. Khim.*, 2002, **28**, 364 [*Coord. Chem.* (*Engl. Transl.*), 2002, **28**].
31. C. Glidewell, M. E. Haman, M. B. Hursthouse, I. L. Johnson, M. Motevalli, *J. Chem. Res.*, 1988, **212**, 1676.
32. J. T. Thomas, J. H. Robetson, E. G. Cox, *Acta Crystallogr.*, 1958, **11**, 599.
33. N. A. Sanina, O. A. Rakova, S. M. Aldoshin, I. I. Chuev, L. O. Atovmyan, N. S. Ovanesyan, *Koord. Khim.*, 2001, **27**, 198 [*Coord. Chem.* (*Engl. Transl.*), 2001, **27**].
34. O. A. Rakova, N. A. Sanina, G. V. Shilov, V. V. Strelets, A. V. Kulikov, S. M. Aldoshin, *Koord. Khim.*, 2001, **27**, 698 [*Coord. Chem.* (*Engl. Transl.*), 2001, **27**].
35. C. Glidewell, R. J. Lambert, M. B. Hursthouse, M. Motevalli, *J. Chem. Soc., Dalton Trans.*, 1989, 2061.
36. O. Jimenez-Sandoval, R-Cea-Olivares, S. Hernandez-Ortega, *Polyhedron*, 1997, **16**, 4129.
37. C. Glidewell, M. E. Harman, M. B. Hursthouse, I. L. Johnson, M. J. Motevalli, *Chem. Research (S)*, 1988, **212**, 1676.
38. T. C. W. Mak, L. Book, C. Chien, M. K. Gallagher, L. C. Song, D. Seyferth, *Inorg. Chim. Acta*, 1983, **73**, 159.
39. R. Cassoly, Q. H. Gibson, *J. Mol. Biol.*, 1975, **91**, 301.
40. E. Antonini, M. Brunori, *Hemoglobin and Myoglobin in the Reactions with Ligands*, in *North-Holland Research Monographs. Fronties of Biology*, Eds A. Neuberger, E. L. Tatum, North-Holland Publishing Company, Amsterdam—London, 1971, 21, 276.
41. A. F. Vanin, *Biokhimiya*, 1998, **63**, 924 [*Biochem.* (*Moscow*) (*Engl. Transl.*), 1998, **63**].
42. K. A. Persall, F. T. Boner, *Inorg. Chem.*, 1982, **21**, 1978.
43. S. V. Lymar, V. Shafirovich, G. A. Poskrebyshev, *Inorg. Chem.*, 2005, **44**, 5212.
44. G. A. Poskrebyshev, V. Shafirovich, S. V. Lymar, *J. Am. Chem. Soc.*, 2004, **126**, 891.

45. M. D. Bartberger, W. Liu, E. Ford, K. M. Miranda, C. Switzer, J. M. Fukuto, P. J. Farmer, D. A. Wink, K. N. Houk, *Proc. Natl. Acad. Sci. USA*, 2002, **99**, 10958.
46. L. M. Blomberg, M. R. A. Blomberg, P. E. M. Siegbahn, *J. Biol. Inorg. Chem*., 2007, **12**, 79.
47. K. Szacilowski, A. Chmura, Z. Stasicka, *Coord. Chem. Rev*., 2005, **249**, 2408.
48. P. G. Wang, M. Xian, X. Tang, X. Wu, Z. Wen, T. Cai, A. J. Janczuk, *Chem. Rev*., 2002, **102**, 1091.
49. S. Costanzo, S. Menage, R. Parello, R. P. Bonomo, M. Fontecave, *Inorg. Chim. Acta*, 2001, **318**, 45.
50. M. Jaworska, Z. Stasicka, *New J. Chem*., 2005, **29**, 604.
51. A. F. Shestakov, Yu. N. Shul´ga, N. S. Emel´yanova, N. A. Sanina, S. M. Aldoshin, *Izv. Akad. Nauk*, *Ser. Khim*., 2007, 1244 [*Russ. Chem. Bull., Int. Ed.*, 2007, **56**, 1289].
52. A. F. Shestakov, S. M. Aldoshin, N. A. Sanina, Yu. M. Shul´ga, *Mendeleev Commun.*, 2004, No. 1, 9.
53. M. Lewin, K. Fisher, I. Dance, *Chem. Commun*., 2000, 947.
54. P. F. Ford, J. Bourassa, K. Miranda, B. Lee, I. Lorkovic, S. Boggs, S. Kudo, L. Laverman, *Coord. Chem. Rev*., 1998, **171**, 185.
55. M. Lewin, K. Fisher, I. Dance, *Chem. Commun*., 2000, 947.

Received June 23, 2006;
in revised form December 29, 2008